0026-895X/01/5902-393–402$3.00
MOLECULAR PHARMACOLOGY
Vol. 59, No. 2
196/880692
Mol Pharmacol 59:393–402, 2001
Printed in U.S.A.

Molecular Mechanisms Controlling the Rate and Specificity of Catechol *O*-Methylation by Human Soluble Catechol *O*-Methyltransferase

PIA LAUTALA,[1] ISMO ULMANEN,[2] and JYRKI TASKINEN

Department of Pharmacy, Viikki Drug Discovery Technology Center, University of Helsinki, Finland (P.L., J.T.) and Orion Pharma, Molecular Biology and Target Protein Research, Viikki Biocenter, Helsinki, Finland (I.U.)

Received April 8, 2000; accepted October 17, 2000

This paper is available online at http://molpharm.aspetjournals.org

ABSTRACT

Molecular mechanisms determining the turn-over rate and specificity of catechol *O*-methylation were studied by combining enzyme kinetic measurements, computational modeling of substrate properties and fitting ligands in a 3D model of the active site of the enzyme. Enzyme kinetic measurements were carried out for 46 compounds, including most clinically used catechol drugs, by using recombinant human soluble catechol *O*-methyltransferase (COMT). The most important mechanism decreasing the turnover rate and increasing affinity was the electron withdrawing effect of substituents. Several other mechanisms by which substituents affected reactivity and affinity were identified. Highest turnover rates were determined for unsubstituted catechol and pyrogallol. Pyrogallol derivatives generally seemed to be more specific substrates than catechols. Catecholestrogens were the most specific endogenous substrates, whereas catecholamines were rather poor substrates. Among the catechol drugs used in the L-DOPA treatment of Parkinson's disease, the COMT inhibitors entacapone and tolcapone were not methylated, whereas the DOPA decarboxylase inhibitor benserazide was 15 times more specific substrate than L-DOPA, the target of COMT inhibition. The structure-activity relationships found allow the prediction of reactivity, affinity, and specificity with useful accuracy for catechols with a wide range of structures and properties. The knowledge can be used in the evaluation of metabolic interactions of endogenous catechols, drugs and dietary catechols, and in the designing of drugs with the catechol pharmacophore.

Methylation of catechols is catalyzed by the enzyme catechol *O*-methyltransferase (COMT, EC 2.1.1.6). The reaction involves the transfer of the activated methyl group of *S*-adenosyl-L-methionine (AdoMet) to one of the catecholic hydroxyls (Männistö et al., 1992). COMT is an enzyme considered to have wide specificity toward catechol type substrates; the only strict requirement was that the substrate must have a vicinal dihydroxyphenyl structure. The most important physiological substrates of COMT are catecholamines, their metabolites, and catecholestrogens. The exogenous substrates include many drugs. In addition to COMT's important role in drug metabolism and interactions, the discovery of it as a possible drug target has remarkably increased the interest in this enzyme during the last few years. Two COMT inhibitor drugs, entacapone and tolcapone, have been recently introduced to enhance the L-DOPA/DOPA decarboxylase (DDC) inhibitor therapy in the treatment of Parkinson's disease (Keränen et al., 1993; Zürcher et al., 1993). All three drugs used in this new combination therapy have a catechol-type structure.

During the intensive search for potent and selective COMT inhibitors, two forms of both human and rat COMT cDNAs have been cloned; the shorter cDNAs coded for the cytoplasmic soluble form (S-COMT) and the longer cDNAs coded for the membrane-bound form (MB-COMT) located in the rough endoplasmic reticulum (Salminen et al., 1990; Bertocci et al., 1991; Lundström et al., 1991; Ulmanen et al., 1997). The recombinant proteins have been produced using an *Escherichia coli* expression system (Lundström et al., 1992; Malherbe et al., 1992; Tilgmann and Ulmanen, 1996), in mammalian cell lines (Bertocci et al., 1991; Lundström et al., 1991; Malherbe et al., 1992; Tilgmann et al., 1992) and in baculovirus-infected insect cells (Tilgmann et al., 1992). The soluble enzyme has been reported to be the predominant

This work was supported by the Biotechnology and Biological Sciences Research Council, the Commission of the European Communities (BMH4-CT97–2621).

[1] Current address: Orion Pharma, Department of Pharmacokinetics, Espoo, Finland.

[2] Current address: National Public Health Institute, Laboratory of Human Molecular Genetics, Helsinki, Finland.

ABBREVIATIONS: COMT, catechol *O*-methyltransferase; AdoMet, *S*-adenosyl-L-methionine; S-COMT, soluble catechol *O*-methyltransferase; MB-COMT, membrane-bound catechol *O*-methyltransferase; MEP, molecular electrostatic potential; DOPA, 3,4-dihydroxyphenylalanine; QSAR, quantitative structure-activity relationships; TOR, turn-over rate; DDC, 3,4-dihydroxyphenylalanine decarboxylase.

form of COMT in most tissues. However, the membrane-bound enzyme predominates in the human brain, the adrenal medulla, and pheochromocytomas (Tenhunen et al., 1994; Eisenhofer et al., 1998).

The three-dimensional structure of rat S-COMT complexed with AdoMet and the inhibitor 3,5-dinitrocatechol has been solved by X-ray crystallography (Vidgren et al., 1994). Rat enzyme is expected to be a good model for human enzyme, because all residues involved in catechol binding and catalysis are conserved. The catalytic machinery and the residues involved in the binding of the catechol ligand are shown in Fig. 1. Based on the crystal structure, the primary mechanism of catechol recognition is supposed to be the coordination of the two hydroxyl oxygens to the Mg^{2+} ion, which is located at the bottom of a shallow groove. Binding to the Mg^{2+} ion positions one of the hydroxyls close to the activated methyl of AdoMet and the amino group of Lys144 located on opposite sides of the catechol ring. The other hydroxyl is hydrogen bonded to a carboxyl oxygen of Glu199. A recent molecular dynamics study suggests that less acidic catechols may prefer a monodentate rather than a bidentate coordination with the magnesium ion (Kuhn and Kollman, 2000). Lys144 is assumed to act as the catalytic base abstracting a proton from the reacting hydroxyl as the first step of the nucleophilic attack of the catecholate oxygen on the methyl carbon. A rather detailed picture of the catalytic mechanism has emerged based on the crystal structure and recent theoretical studies (Zheng and Bruice, 1997; Ovaska and Yliniemelä, 1998; Lau and Bruice, 1998; Kuhn and Kollman, 2000). However, the effect of the substrate structure on the catalytic rate and selectivity of the reaction is not well understood.

As a part of a larger collaborative work on catechol conjugation, we have studied the effect of the molecular structure on the methylation reaction catalyzed by human S-COMT. Enzyme kinetics were studied for 46 catechols representing a variety of structural types and physical-chemical properties and most of the clinically used catechol-type drugs. Kinetic analysis, computational studies on substrates, and modeling of interactions in the active site were combined to elucidate the molecular mechanisms responsible for specificity and efficiency of reaction and to build simple empirical models and rules that make possible the evaluation of turn-over rates and affinities from the molecular structure with useful accuracy.

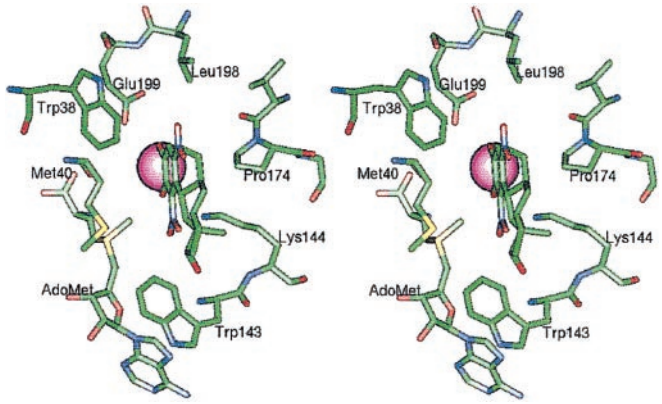

Fig. 1. A stereoview of the active site of catechol *O*-methyltransferase with 2-hydroxyestradiol superimposed on the complexed inhibitor, 3,5-dinitrocatechol. Crystal coordinates of rat S-COMT are from Brookhaven Protein Data Bank entry 1VID (Vidgren et al., 1994). The catechol hydroxyls are coordinated to Mg^{2+} shown as the CPK ball.

Materials and Methods

Chemicals and Enzymes. The catecholic compounds were purchased from Aldrich (Steinheim, Germany), Apin (Abingdon, UK), ICN (Costa Mesa, CA), Merck (Darmstadt, Germany), and Sigma (St. Louis, MO), and were of the highest grade available. Entacapone, tolcapone, 3-nitrocatechol, and 3,5-dinitrocatechol were kind gifts from Orion Pharma (Espoo, Finland). The recombinant human and rat soluble catechol *O*-methyltransferases were produced in *E. coli* as described previously (Lundström et al., 1992). The protein concentrations of the bacterial cell lysates were determined as described using bovine serum albumin as a reference standard (Bradford, 1976). The cell lysates were divided into small aliquots and stored at −70°C before being used. Each aliquot was thawed only once and used immediately for the assays. A validation study showed that the day-to-day reproducibility of V_{max} (concentration of active enzyme) is better than 4% using this procedure (Lautala et al., 1999).

Enzyme Assay. The apparent kinetic constants were determined by varying the catechol concentration at a fixed concentration of AdoMet (150 μM; Roche Diagnostics, Mannheim, Germany). The range of six substrate concentrations (each in duplicate) was selected separately for each catechol. The reactions were carried out in 100 mM Na_2HPO_4/NaH_2PO_4 buffer, pH 7.4, containing 5 mM $MgCl_2$, 20 mM L-cysteine, and 0.2 to 20 μg of protein from the cell lysates in a total volume of 100 μL. To quantify the methylated products, 0.1 μCi of *S*-adenosyl-L-[*methyl*-^{14}C]methionine (NEN, DuPont, Boston, MA) was added into each sample. The amount of protein was chosen for each substrate based on the concentration range used to maintain appropriate experimental conditions for Michaelis-Menten kinetics. The samples were preincubated for 5 min at 37°C before the reactions were initiated by adding the AdoMet/[^{14}C]AdoMet mixture. After an additional 15-min incubation period, the reactions were terminated by adding 10 μL of cold 4 M perchloric acid. The precipitated proteins were removed by centrifugation (14,000 rpm, 5 min).

Inhibition Studies. The K_m values for 3,4-dihydroxybenzoic acid ethyl ester, 4-nitrocatechol, 3-nitrocatechol, and tetrachlorocatechol were determined as K_i values for competitive inhibition. The methylation velocity of 3,4-dihydroxybenzoic acid or 6,7-dihydroxycoumarin was measured at six different initial concentrations of the substrate (5–300 μM and 0.05–5 μM, respectively) in the presence of variable concentrations of the inhibitor. The K_i values were determined similarly for 2,3-dihydroxybenzoic acid and apomorphine.

High-Performance Liquid Chromatography. Quantification of the methylated products was achieved by high-performance liquid chromatography (1090; software HP Chemstation, version 2.1.5; Hewlett Packard, Waldbronn, Germany) connected to a flow scintillation analyzer (150TR; Packard, Meriden, CT). The analyzer was fitted with either a 300-μL cell packed with silanized, cerium-activated lithium glass as scintillant or a 500-μL cell into which 3 ml/min of scintillation liquid (Monoflow 3; National Diagnostics, Atlanta, GA) was pumped. The separation was achieved by the method of Lautala et al. (1999) using a Hypersil BDS-C18 column (125 × 4 mm, 5 μm; Hewlett Packard) and a mixture of phosphate/citrate buffer (50 mM Na_2HPO_4, 20 mM citric acid, 0.15 mM Na_2EDTA, pH adjusted to 3.2 with *O*-phosphoric acid) and methanol. When basic groups containing compounds were analyzed, 1.25 mM 1-octanesulfonic acid was added to the above-mentioned buffer. The amount of methanol in the mobile phase varied between 3 and 60%, depending on the catechol substrate. The mobile phase flow rate was 1.0 ml/min and the oven temperature was set at 40°C. Injection volume was 100 μL. When 6,7-dihydroxycoumarin was used as the substrate in inhibition studies, the formation rate of the reaction product, scopoletin, was measured by a Hewlett Packard liquid chromatograph, model 1100, using a Hypersil BDS-C18 column (250 × 4 mm, 5 μm, Hewlett Packard). The mobile phase consisted of a 50 mM

NaH_2PO_4 buffer, pH 3.0 and methanol (27/73, v/v). The mobile phase flow rate was 1.0 ml/min and the oven temperature was 40°C. Scopoletin was detected using a fluorescence detector (RF-535; Shimadzu, Kyoto, Japan) set at excitation and emission wavelengths of 335 and 455 nm, respectively. Quantification was performed with the aid of a reference standard.

Kinetic Analysis. The kinetic data was analyzed by fitting the Michaelis-Menten equation to the initial velocities obtained using the Leonora Steady-State Enzyme Kinetics program version 1.0 by Cornish-Bowden (Oxford University Press, UK). The K_i values were determined by fitting the rate equations for competitive, uncompetitive, and mixed inhibition to the data.

Molecular Modeling and QSAR. Catechol ligands were modeled using Spartan 5.0 program (Wavefunction Inc., Irvine, CA), and the structures were optimized with the use of the semiempirical AM1 method. Conformational analysis was carried out for hydrocaffeic acid (**26**) and dopamine (**27**) using the coordinate driving function of Spartan. The two side chain C-C bonds of these compounds were rotated in 30° increments. Conformers were AM1-optimized with the two dihedrals constrained. Molecular electrostatic potentials (MEP) were computed for the AM1-optimized structures by single-point, ab initio calculations at the 3–21G(*) level. For selected compounds, calculations were carried out at the 6–31+G* level. Because no essential improvement was achieved for the purposes of this study, the lower level was chosen to keep the computational cost compatible for QSAR type of work. Two MEP parameters were used in the QSAR analysis: MEP_{vdW}, the minimum value of MEP (kcal/mol) on an electron density isosurface (0.002 electrons/au^3), and MEP_{vol}, the volume (Å^3) of the isoenergy MEP surface at −160 kcal/mol. Catechols were modeled in the active site of the crystal structure of rat S-COMT (Brookhaven Protein Data Bank entry 1VID) using Insight II program (Molecular Simulations, Inc., San Diego, CA). The ligand structures were superimposed on the dinitrocatechol inhibitor in the crystal structure of rat S-COMT with the catechol hydroxyls coordinated to the magnesium ion. The effect of monodentate binding geometry was evaluated by keeping the reacting hydroxyl in the fixed position and tilting the molecule in the aromatic plane. Several low-energy conformers of flexible ligands were studied. Energy minimization of the complexes was not carried out because of the difficulties of molecular mechanics force fields to deal with the Mg^{2+} chelation and the electronic substituent effects. Octanol-water distribution coefficients were calculated with the use of the LOGKOW method (Meylan and Howard, 1995), and SPSS 8.0.1 program (SPSS Inc., Chicago, IL) was used for statistical analyses. Cross-validation of regression models was carried out by leaving out five randomly selected compounds and predicting a value for them using a model build without the rest of the set. The prediction residuals were used for calculating cross-validated R^2.

Results

Methylation Kinetics. A set of 46 catecholic compounds (Fig. 2) was selected for the enzyme kinetic study to elucidate turnover rate (TOR), binding affinity and specificity in the reaction catalyzed by human soluble COMT. Initial velocity for the formation of the methylated product was studied as the function of catechol concentration. The reaction velocities were measured using a ^{14}C-labeled cosubstrate, *S*-adenosyl-L-methionine, and high-performance liquid chromatography with on-line radioactivity detector. The apparent V_{max}, K_m, and V_{max}/K_m values were obtained by fitting the Michaelis-Menten equation to the initial velocity data (Table 1). It was not possible to determine a proper kinetic curve in the case of four compounds (4-nitrocatechol, 3-nitrocatechol, tetrachlorocatechol, and 6,7-dihydroxycoumarin) which exhibited very low reactivity and high affinity. The K_m value for these compounds was determined as the K_i value for competitive inhibition. The V_{max} value was approximated by the highest activity measured.

Formation of two products, corresponding to the two monomethylated regioisomers, was observed with many substrates. However, the analytical method using the ^{14}C labeled cosubstrate did not allow determination of the preferred methylation site of the various compounds. Kinetic analysis was made for the formation of each product, if both were abundant enough. The sum of V_{max} values was used to calculate the turnover rate for substrate consumption relative to the nonsubstituted catechol (Table 2). Similarly, the sum of V_{max}/K_m values was used to calculate the specificity constant k_A, which determines the ratio of rates of competing substrates when they are mixed together (Cornish-Bowden, 1995), relative to catechol.

The highest turnover rates were found for catechol and pyrogallol, both about 50 nmol/min/mg. The turn-over rate of all the other compounds was lower than that of nonsubstituted catechol. The lowest value that could be determined was about 0.2 nmol/min/mg for 3-nitrocatechol. The K_m values varied by 5 orders of magnitude, from 0.02 μM for 3-nitrocatechol to 1800 μM for α-methyl-DOPA. The K_m value of catechol was 50 μM. The most specific substrates were 2,3-dihydroxynaphthalene and tetrachlorocatechol, which exhibited a 20-fold specificity constant (k_A) compared with that of catechol. Catecholamine derivatives and DOPA derivatives were less specific substrates than catechol. The most specific endogenous substrate was 2-hydroxyestradiol with relative $k_A = 12$. Among drugs used in the treatment of Parkinson's disease, benserazide showed equal V_{max} and K_m values with catechol, whereas L-DOPA and carbidopa were poor substrates with the respective V_{max}/K_m values of 0.053 and 0.024 ml/min/mg, and the COMT inhibitors entacapone and tolcapone were not detectably methylated. Other compounds that did not react at a measurable rate were 3,5-dinitrocatechol, 2,3-dihydroxybenzoic acid, and apomorphine. Binding of apomorphine and 2,3-dihydroxybenzoic acid in the active site was studied by measuring their effect on the initial methylation velocity of 3,4-dihydroxybenzoic acid as the function of substrate and inhibitor concentration. The data were best-fitted to the equation for mixed inhibition. The K_{ic} and K_{iu} values were 241 μM and 3110 μM for apomorphine and 378 μM and 6736 μM for 2,3-dihydroxybenzoic acid, respectively. 3,5-Dinitrocatechol, entacapone, and tolcapone are known as tight-binding competitive inhibitors of COMT; the published K_i value for entacapone and tolcapone was 0.3 nM (Lotta et al., 1995).

Methylation by rat recombinant S-COMT was studied for 22 compounds to evaluate the appropriateness of the rat enzyme as a model for human S-COMT (Table 3). The K_m values for human and rat enzymes were highly correlated ($r^2 = 0.988$, $n = 25$, including regioisomers), but the K_m values for the rat enzyme were 3 to 4 times higher, on average. The V_{max} values were also highly correlated ($r^2 = 0.927$, $n = 25$). The absolute values of human and rat V_{max} were not comparable, because accurate concentrations of the active enzyme were not known.

Factors Governing Reactivity and Affinity. The effect of substrate structure on binding and catalysis was studied by analyzing the correlation of enzyme kinetic parameters

with the properties of substrates and their interactions with the enzyme structure.

Electronic substituent effect on the reacting hydroxyl was studied first with compounds **1** to **8**, which have a small substituent in the 4-position with minimal direct interactions with the binding site. Hammet σ^- constants have been derived based on the effect of substituents on the ionization of substituted phenols (Perrin et al., 1981). High correlation (r^2 = 0.94) was found between the turnover rate and Hammet σ_p^-, which quantifies the effect of a *para* substituent on the pK_a value of a phenolic hydroxyl, the turnover rate decreasing with increased ionization. Hammet constants, however, are available only for a limited set of structures. As an alternative parameter for prediction of the electronic effect, we studied the use of the molecular electrostatic potential, which can be readily calculated for any structure. In a pre-

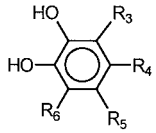

Compound	R3	R4	R5	R6
1 Catechol	H	H	H	H
2 4-Methylcatechol	H	CH_3	H	H
3 4-Isopropylcatechol	H	$CH(CH_3)_2$	H	H
4 4-*tert*-Butylcatechol	H	$C(CH_3)_3$	H	H
5 4-Chlorocatechol	H	Cl	H	H
6 3,4-Dihydroxyacetophenone	H	$COCH_3$	H	H
7 3,4-Dihydroxybenz. ac. ethyl ester	H	$COOCH_2CH_3$	H	H
8 4-Nitrocatechol	H	NO_2	H	H
9 4-*tert*-Butyl-5-methoxycatechol	H	$C(CH_3)_3$	OCH_3	H
10 Pyrogallol	OH	H	H	H
11 3-Nitrocatechol	NO_2	H	H	H
12 3-Fluorocatechol	F	H	H	H
13 3-Methoxycatechol	OCH_3	H	H	H
14 3-Methoxy-5-bromocatechol	OCH_3	H	Br	H
15 Methylgallate	OH	H	$COOCH_3$	H
16 Benserazide	OH	$CH_2NHNHCOCH(NH_2)CH_2OH$	H	H
17 3,5-Dinitrocatechol	NO_2	H	NO_2	H
18 Tolcapone	NO_2	H	$COC_6H_4CH_3$	H
19 Entacapone	NO_2	H	$CH=C(CN)CON(CH_2CH_3)_2$	H
20 3,4-Dihydroxybenzoic acid	H	COOH	H	H
21 2,3-Dihydroxybenzoic acid	COOH	H	H	H
22 3,4-Dihydroxyphenyl acetic acid	H	CH_2COOH	H	H
23 3,4-Dihydroxymandelic acid	H	CH(OH)COOH	H	H
24 3,4-Dihydroxyphenylglycol	H	$CH(OH)CH_2(OH)$	H	H
25 Caffeic acid	H	CH=CHCOOH	H	H
26 Hydrocaffeic acid	H	CH_2CH_2COOH	H	H
27 Dopamine	H	$CH_2CH_2NH_2$	H	H
28 5-Hydroxydopamine	H	$CH_2CH_2NH_2$	H	OH
29 6-Hydroxydopamine	H	$CH_2CH_2NH_2$	OH	H
30 L-Noradrenaline	H	$CH(OH)CH_2NH_2$	H	H
31 L-Adrenaline	H	$CH(OH)CH_2NHCH_3$	H	H
32 Isoprenaline	H	$CH(OH)CH_2NHCH(CH_3)_2$	H	H
33 Dobutamine	H	$(CH_2)_2NHCH(CH_3)(CH_2)_2C_6H_4OH$	H	H
34 L-dopa	H	$CH_2CH(NH_2)COOH$	H	H
35 α-Methyldopa	H	$CH_2C(NH_2)(CH_3)COOH$	H	H
36 S(-)-Carbidopa	H	$CH_2C(NHNH_2)(CH_3)COOH$	H	H
37 L-dopa methylester	H	$CH_2CH(NH_2)COOCH_3$	H	H
38 Tetrachlorocatechol	Cl	Cl	Cl	Cl

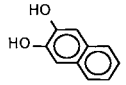

39 2,3-Dihydroxynaphthalene

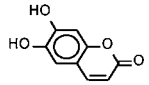

40 6,7-Dihydroxycoumarin

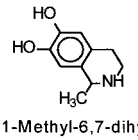

41 1-Methyl-6,7-dihydroxy-1,2,3,4-tetrahydroisoquinoline

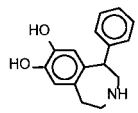

42 SKF-38393

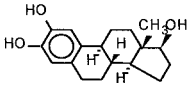

43 2-Hydroxyestradiol

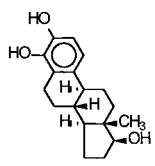

44 4-Hydroxyestradiol

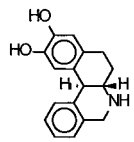

45 Dihydrexidine

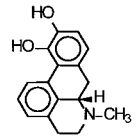

46 Apomorphine

Fig. 2. Structural formulae of the studied catechols.

liminary study, MEPs of catechols **1** to **8** were calculated at different protonation states, neutral, monoanionic (two forms in the case of asymmetrically substituted catechols), and dianionic catechol function. Two descriptors, MEP_{vdW}, the minimum value of MEP on an electron density isosurface, and MEP_{vol}, the volume of an isoenergy MEP surface, were used in the correlation analysis. The catecholate monoanion with the higher MEP minimum was found to be the only species giving MEP descriptors correlated with enzyme kinetic parameters. The MEP isoenergy surfaces plotted at −160 kcal/mol are shown for catechol and 4-nitrocatechol in Fig. 3. In the training set of compounds **1** to **8**, the turnover rate was directly proportional to MEP_{vol}, which explained 98% of its variation. Correlation between TOR and MEP_{vol}

TABLE 1
Apparent enzyme kinetic parameters for the methylation of catechols catalyzed by recombinant human soluble catechol *O*-methyltransferase[a]

	Compound	V_{max}	K_m	V_{max}/K_m
		nmol/min/mg	*μM*	*ml/min/mg*
1	Catechol	48.9 ± 0.9	49.7 ± 1.6	0.98
2	4-Methylcatechol	24.4 ± 0.9	29.1 ± 3.9	0.84
		23.3 ± 1.1	36.7 ± 3.3	0.63
3	4-Isopropylcatechol	36.3 ± 1.7	26.1 ± 3.0	1.39
		6.9 ± 1.5	40.5 ± 27.4	0.17
4	4-*tert*-Butylcatechol	41.9 ± 2.7	31.9 ± 8.0	1.31
5	4-Chlorocatechol	36.0 ± 0.1	11.7 ± 0.5	3.08
6	3,4-Dihydroxyacetophenone	9.8 ± 0.7	1.4 ± 0.3	7.00
7	3,4-Dihydroxybenz.ac.ethyl ester	7.2 ± 1.7	0.66 ± 0.17	10.9
		3.5 ± 1.1	0.66 ± 0.17	5.30
8	4-Nitrocatechol	0.77 ± 0.09	0.12 ± 0.02	6.42
		0.78 ± 0.05	0.12 ± 0.02	6.50
9	4-*tert*-Butyl-5-methoxycatechol	32.5 ± 2.4	18.5 ± 2.3	1.76
10	Pyrogallol	53.2 ± 1.5	10.4 ± 0.6	5.12
11	3-Nitrocatechol	0.15 ± 0.02	0.020 ± 0.001	7.50
12	3-Fluorocatechol	30.7 ± 1.8	7.8 ± 1.0	3.94
13	3-Methoxycatechol	39.8 ± 1.8	24.5 ± 2.8	1.62
14	3-Methoxy-5-bromocatechol	17.3 ± 0.9	2.5 ± 0.4	6.92
15	Methylgallate	11.7 ± 0.4	1.0 ± 0.1	11.7
16	Benserazide	41.8 ± 3.6	50.2 ± 7.2	0.83
17	3,5-Dinitrocatechol	N.D.[b]		
18	Tolcapone	N.D.		
19	Entacapone	N.D.		
20	3,4-Dihydroxybenzoic acid	35.6 ± 0.9	19.9 ± 2.0	1.79
		7.7 ± 0.1	28.3 ± 0.4	0.27
21	2,3-Dihydroxybenzoic acid	N.D.		
22	3,4-Dihydroxyphenyl acetic acid	34.0 ± 2.2	68.8 ± 10.8	0.49
		4.0 ± 0.1	53.7 ± 4.0	0.074
23	3,4-Dihydroxymandelic acid	43.7 ± 2.0	132 ± 11	0.33
24	3,4-Dihydroxyphenylglycol	37.2 ± 1.4	46.4 ± 4.7	0.80
25	Caffeic acid	25.9 ± 1.9	3.2 ± 0.7	8.09
		15.5 ± 0.2	2.8 ± 0.1	5.54
26	Hydrocaffeic acid	31.5 ± 1.7	25.4 ± 4.5	1.24
		12.1 ± 0.03	45.1 ± 0.3	0.27
27	Dopamine	35.9 ± 1.4	188 ± 16	0.19
28	5-Hydroxydopamine	46.7 ± 1.1	61.6 ± 4.1	0.76
29	6-Hydroxydopamine	25.3 ± 2.0	244 ± 32	0.10
30	L-Noradrenaline	33.2 ± 0.8	256 ± 20	0.13
31	L-Adrenaline	44.0 ± 1.0	132 ± 13	0.33
32	Isoprenaline	25.8 ± 0.6	145 ± 8.5	0.18
		3.1 ± 0.3	170 ± 31	0.018
33	Dobutamine	29.0 ± 0.9	23.7 ± 3.1	1.22
		6.9 ± 0.5	28.6 ± 7.5	0.24
34	L-DOPA	29.8 ± 0.9	564 ± 28	0.053
35	α-Methyl-DOPA	21.4 ± 0.7	1789 ± 108	0.012
		2.6 ± 0.3	1170 ± 309	0.002
36	*S*(−)-Carbidopa	14.3 ± 0.8	599 ± 63	0.024
37	L-DOPA methyl ester	44.2 ± 0.7	51.1 ± 2.9	0.86
38	Tetrachlorocatechol	0.62 ± 0.03	0.029 ± 0.002	21.4
39	2,3-Dihydroxynaphthalene	30.8 ± 1.6	1.5 ± 0.3	20.5
40	6,7-Dihydroxycoumarin	3.3 ± 0.03	0.30 ± 0.01	11.0
41	1-Methyl-6,7-dihydroxy-1,2,3,4-tetrahydroisoquinoline	18.3 ± 0.9	29.4 ± 3.7	0.62
		10.6 ± 0.1	36.2 ± 0.2	0.29
42	SKF 38393	5.0 ± 0.04	67.2 ± 1.2	0.074
		10.5 ± 0.5	73.6 ± 8.3	0.14
43	2-Hydroxyestradiol	32.4 ± 2.6	3.7 ± 1.1	8.76
		13.7 ± 1.8	4.2 ± 2.2	3.26
44	4-Hydroxyestradiol	31.5 ± 2.5	12.4 ± 2.6	2.54
45	Dihydrexidine	10.1 ± 2.3	25.0 ± 14.5	0.40
		10.5 ± 6.2	53.1 ± 50.6	0.20
46	Apomorphine	N.D.		

[a] The enzyme kinetic parameters were determined as described under *Materials and Methods.*
[b] N.D., no methylation detected; the highest substrate concentration tested was 500 μM.

for a larger subset of compounds with no ionizable substituents was $r^2 = 0.932$ ($n = 20$) (Fig. 4). The only outlier was 3-nitrocatechol, which has a nitro-group in the *ortho*-position to the ionized hydroxyl. When the compounds containing amino and carboxyl groups were included, the correlation deteriorated clearly ($r^2 = 0.705$, $n = 38$) (Fig. 4). Two more outliers were also found: 3,4-dihydroxybenzoic acid (**20**) and caffeic acid (**25**), which have a carboxyl group conjugated with the aromatic system.

K_m values were found to depend on the ionization of the catechol function as well. In the training set of compounds **1** to **8,** Hammet σ_p^- and MEP_{vol} explained 94 and 97% of the variation in $\log(1/K_m)$, respectively. In the whole data set (three outliers removed), MEP_{vol} explained only 59% of the variation in $\log(1/K_m)$ values. Octanol-water distribution coefficient $logK_{ow}$ combined with the electronic parameter produced a highly significant regression model explaining more than 80% of the variation: $\log(1/K_m) = -0.30 (\pm 0.03) MEP_{vol} + 0.21 (\pm 0.03) logK_{ow} + 6.99 (\pm 0.23)$ [$n = 38$; $R^2 = 0.833$; $s = 0.434$; $F = 87.5$].

The hydrophobicity parameter $logK_{ow}$ was calculated for the ionized form of side chain, when appropriate. Predictive ability of the model was evaluated by leave-five-out cross-validation, which gave $R^2 = 0.782$. The data used in the QSAR analysis and the fitting results are shown in Table 2. Correlation of the experimental values and $\log(1/K_m)$ values calculated by eq. 1 are shown in Fig. 5. Largest errors were observed for α-methyl-DOPA (**35**) and carbidopa (**36**), the affinity of which was overestimated by 1 order of magnitude.

Steric and hydrophobic effects were evaluated at structural level by analyzing the overlapping of ligand and enzyme structures, and van der Waals contacts of hydrophobic and polar areas of the ligand surface, when superimposed on the inhibitor in the crystal structure of rat S-COMT (Fig. 1). The 5-nitro group of the inhibitor is sandwiched between the "gate-keeper" residues Pro174 and Trp38, π electrons of the conjugated substituent apparently having favorable interactions with a Pro174 methylene and the edge of Trp38 aromatic ring. Compounds with a planar conjugated substituent in the 4-position or a 4,5-fused aromatic ring (4-nitrocatechol, 2,3-dihydroxynaphthalene, 6,7-dihydroxycoumarin, caffeic acid, and 3,4-dihydroxybenzoic acid) have a fit of the substituent similar to that of the 5-nitro group of the inhibitor. Approximately planar saturated ring structures attached to the 4,5-position, such as the steroid nucleus of 2-hydroxyestradiol, have extended tight contacts with Pro174 and Trp38. The ring systems of dihydrexidine and SKF38393

TABLE 2

Relative TOR $(\Sigma V_{max})_{regioisomers}/(V_{max})_{catechol}$ and specificity constants $(k_{A(rel)})$ $(\Sigma V_{max}/K_m)_{regioisomers}/(V_{max}/K_m)_{(catechol)}$ for substrate consumption catalyzed by human S-COMT, and the data used in the QSAR analysis

Compound	TOR	$k_{A(rel)}$	MEP_{vol}[a]	$LogK_{ow}$[b]	$Log(1/K_m)_{obs}$[c]	$Log(1/K_m)_{calc}$[d]	Residual
Catechol	1.00	1.00	9.11	1.03	4.30	4.19	0.11
4-Methylcatechol	0.98	1.50	8.78	1.58	4.54	4.41	0.13
4-Isopropylcatechol	0.88	1.59	8.33	2.49	4.58	4.74	−0.15
4-*tert*-Butylcatechol	0.86	1.34	8.08	2.94	4.5	4.91	−0.41
4-Chlorocatechol	0.74	3.14	6.07	1.68	4.93	5.24	−0.30
3,4-Dihydroxyacetophenone	0.20	7.14	3.06	0.71	5.85	5.93	−0.07
3,4-Dihydroxybenzoic acid ethyl ester	0.22	16.5	2.8	1.36	6.18	6.14	0.04
4-Nitrocatechol	0.032	13.2	0.99	1.43	6.92	6.69	0.23
4-*tert*-Butyl-5-methoxycatechol	0.66	1.80	6.73	3.02	4.73	5.32	−0.59
Pyrogallol	1.09	5.22	9.16	1.23	4.98	4.22	0.76
3-Fluorocatechol	0.63	4.02	7.33	0.97	5.11	4.71	0.40
3-Methoxycatechol	0.81	1.65	7.29	0.86	4.61	4.70	−0.09
3-Methoxy-5-bromocatechol	0.35	7.06	4.49	1.75	5.59	5.72	−0.14
Methyl gallate	0.24	11.9	2.75	0.81	6.00	6.04	−0.04
Benserazide	0.85	0.85	7.53	−4.70	4.30	3.44	0.86
3,4-Dihydroxyphenyl acetic acid	0.78	0.58	6.36	−3.00	4.16	4.15	0.01
3,4-Dihydroxymandelic acid	0.89	0.34	6.36	−4.02	3.88	3.94	−0.06
3,4-Dihydroxyphenylglycol	0.76	0.82	7.79	−0.53	4.33	4.25	0.08
Hydrocaffeic acid	0.89	1.54	6.09	−2.49	4.60	4.34	0.26
Dopamine	0.73	0.19	7.86	−2.58	3.73	3.80	−0.07
5-Hydroxydopamine	0.96	0.78	8.11	−2.64	4.21	3.71	0.50
6-Hydroxydopamine	0.52	0.10	7.21	−3.07	3.61	3.89	−0.27
L-Noradrenaline	0.68	0.13	7.89	−4.12	3.59	3.46	0.13
L-Adrenaline	0.90	0.34	7.79	−3.58	3.88	3.60	0.27
Isoprenaline	0.59	0.20	7.74	−2.67	3.84	3.81	0.03
Dobutamine	0.73	1.49	7.55	0.59	4.64	4.56	0.08
L-DOPA	0.61	0.054	7.66	−3.4	3.25	3.68	−0.43
α-Methyl-DOPA	0.49	0.014	6.94	−2.95	2.75	3.99	−1.24
S(−)-Carbidopa	0.29	0.024	5.89	−3.31	3.22	4.23	−1.00
L-DOPA methyl ester	0.90	0.88	7.66	−1.96	4.29	3.99	0.30
Tetrachlorocatechol	0.013	21.8	2.05	3.61	7.52	6.84	0.68
2,3-Dihydroxynaphthalene	0.63	20.9	4.82	2.21	5.82	5.72	0.10
6,7-Dihydroxycoumarin	0.067	11.2	1.14	0.55	6.52	6.46	0.06
1-Methyl-6,7-dihydroxy-1,2,3,4-tetrahydroisoquinoline	0.59	0.93	7.67	−1.90	4.53	4.00	0.53
SKF-38393	0.32	0.22	7.59	−0.48	4.13	4.32	−0.19
2-Hydroxyestradiol	0.94	12.3	7.04	3.46	5.43	5.33	0.11
4-Hydroxyestradiol	0.64	2.59	7.02	3.46	4.91	5.33	−0.43
Dihydrexidine	0.42	0.61	6.08	−0.47	4.60	4.78	−0.17

[a] The volume of the isoenergy molecular electrostatic potential surface at −160 kcal/mol.
[b] Octanol-water partitioning parameter for the ionized side chain form of the compounds calculated using LOGKOW method (Meylan and Howard, 1995).
[c] $Log(1/K_m)$ values observed.
[d] $Log(1/K_m)$ values calculated by equation under Factors Governing Reactivity and Affinity.

turn toward the binding site and part of them overlap with the protein.

Substituents *ortho* to a catechol hydroxyl are buried in the hydrophobic binding pocket and have less space available. Small substituents, such as halogens, and a methoxy group can be accommodated; the carboxyl group takes the same space as the 3-nitro group of the inhibitor. The saturated ring system of 4-hydroxyestradiol is attached to the *ortho-meta*-position and overlaps slightly with the enzyme and AdoMet. The phenyl ring in the 3-position of apomorphine overlaps heavily with AdoMet and Trp143.

Polar surfaces of ligands contacting hydrophobic binding site walls, especially ionic groups and hydrogen bond donors, are expected to have an unfavorable effect on binding. Polar groups fixed close to contact distance, or with limited freedom to avoid contact, include a third hydroxyl in the catechol ring, hydroxyl in the β-carbon of catecholamines and their metabolites, and charged groups in the crowded α-carbon of α-methyl-DOPA and carbidopa.

Compounds with flexible substituents and no steric hindrance can adapt their conformation on binding to avoid unfavorable interactions. Dopamine, with a positively charged amino group and hydrocaffeic acid, with carboxylate anion in the two carbon side chains have, in principle, similar flexibility. Hydrocaffeic acid has similar K_m values with 4-methylcatechol, whereas the K_m of dopamine is almost 1 order of magnitude higher. To get insight into the effects of flexibility, conformational analysis was carried out for dopamine and hydrocaffeic acid. Rotating the first two side chain C-C bonds in 30° increments produced 27 conformations of dopamine and 31 conformations of hydrocaffeic acid with AM1 energies less than 4 kcal/mol above the minimum. In the case of dopamine, most of the low energy conformations have *gauche*-geometry (Fig. 6). The *gauche*-conformations of dopamine tended to have the amino group out of the catechol plane, in contact with the hydrophobic protein side chains Pro174 or Trp38, when docked in the enzyme. In the case of hydrocaffeic acid, most low-energy conformations showed *trans*-geometry with the extended side chain pointing out of the binding pocket. Low energy *gauche*-conformations of hydrocaffeic acid tended to have the charged group close to the catechol plane with fewer contacts with the binding site. The cyclic dopamine analog **41** has a K_m value comparable with that of hydrocaffeic acid. Its saturated ring, but also the amino-group, is fixed between Pro174 and Trp38.

Discussion

The V_{max} values observed for unsubstituted catechol and pyrogallol may represent the upper limit of the rate for the methylation catalyzed by human S-COMT. The maximal turnover rate may be limited by factors that are not affected by structural changes in the catechol substrate (e.g., the rather large conformational changes of the protein, which presumably accompany AdoMet binding and *S*-adenosyl-L-homocysteine release). The V_{max} values determined for catechol and pyrogallol was estimated to correspond to a k_{cat} value of 50 to 70/min by comparing the relative substrate turnover rates and the k_{cat} values determined earlier for dopamine, L-DOPA, and 3,4-dihydroxybenzoic acid (Lotta et al., 1995). Absolute k_{cat} values were not determined in this work, because the interest was in changes caused by struc-

TABLE 3
Apparent enzyme kinetic parameters for the methylation of catechols catalyzed by recombinant rat soluble catechol *O*-methyltransferase[a]

	Compound	V_{max}	K_m	V_{max}/K_m
		nmol/min/mg	*μM*	*ml/min/mg*
1	Catechol	184 ± 10	250 ± 22	0.74
2	4-Methylcatechol	82.8 ± 5.7	124 ± 17	0.67
		97.6 ± 6.4	156 ± 20	0.63
3	4-Isopropylcatechol	155 ± 7	75.3 ± 11.8	2.06
		50.0 ± 4.9	104 ± 28	0.48
4	4-*tert*-Butylcatechol	156 ± 6	99.9 ± 7.5	1.56
5	4-Chlorocatechol	138 ± 4	20.3 ± 1.1	6.80
7	3,4-Dihydroxybenz.ac.ethyl ester	28.4 ± 1.4	2.3 ± 0.5	12.3
		15.9 ± 0.3	2.4 ± 0.2	6.63
8	4-Nitrocatechol	3.2 ± 0.1	<5.0	>0.64
		5.9 ± 0.9	<5.0	>1.18
16	Benserazide	134 ± 3	105 ± 6	1.28
17	3,5-Dinitrocatechol	N.D.[b]		
18	Tolcapone	N.D.		
19	Entacapone	N.D.		
20	3,4-Dihydroxybenzoic acid	110 ± 0.1	97.0 ± 0.5	1.13
		23.8 ± 0.8	71.7 ± 9.2	0.33
21	2,3-Dihydroxybenzoic acid	N.D.		
22	3,4-Dihydroxyphenyl acetic acid	90.6 ± 3.0	275 ± 19	0.33
		8.3 ± 2.0	180 ± 132	0.046
27	Dopamine	133 ± 1	826 ± 28	0.16
34	L-DOPA	104 ± 7	1870 ± 193	0.056
36	*S*(−)-Carbidopa	53.1 ± 2.5	1988 ± 129	0.027
39	2,3-Dihydroxynaphthalene	121 ± 11	3.2 ± 0.7	37.8
43	2-Hydroxyestradiol	95.8 ± 0.8	14.3 ± 0.4	6.70
		61.4 ± 9.9	15.0 ± 7.7	4.09
44	4-Hydroxyestradiol	86.9 ± 2.2	27.5 ± 2.3	3.16
45	Dihydrexidine	50.1 ± 3.1	29.9 ± 7.5	1.68
		23.6 ± 2.9	32.0 ± 13.3	0.74
46	Apomorphine	N.D.		

[a] The enzyme kinetic parameters were determined as described under *Materials and Methods*.
[b] N.D., no methylation detected, the highest substrate concentration tested was 500 μM.

tural factors. The sign and magnitude of substituent effects can be readily seen from the relative values.

Three distinct structural factors that may cause lowering of the rate or inhibition of the reaction were identified. The most prevalent among the compounds studied was the electron withdrawing substituent effect, or the ability of the structure to facilitate electron delocalization. This property stabilizes the catecholate anion, leading to lowering of pK_a value of the catechol hydroxyls. Increased ionization of the catecholic hydroxyls evidently increases the free energy of binding of the Michaelis complex. This may be related to changing the binding geometry from monodentate to bidentate coordination with magnesium ion with increased catechol ionization, as suggested by a recent molecular dynamics work (Kuhn and Kollman, 2000). A central principle in enzyme catalysis is the stabilization of the transition state rather than the intermediate complex. In the case of COMT, charge is annihilated rather than created in the transition state (Kuhn and Kollman, 2000). Stabilization of the catecholate anion evidently leads to stabilization of the Michaelis complex at the expense of the transition state complex, and therefore to increase of the activation energy. Similar rationalization has been used to explain the high affinity and lack of reactivity of nitrocatechol COMT inhibitors (Ovaska and Yliniemelä, 1998).

The electronic effect on ionization of the catechol hydroxyls can be predicted for most compounds using the MEP parameter. The parameter works best for neutral compounds. On the other hand, charged substituents attached to the catechol ring through a saturated carbon chain are expected to have a rather small effect on the acidity of the catechol hydroxyls. The turnover rate can be simply predicted to be close to that of unsubstituted catechol (TOR 0.7–1.1) for all compounds with substituents attached to the catechol ring through a sp^3 carbon or oxygen.

Two cases were found in which the MEP parameters did not correlate with the expected substituent effect on ioniza-

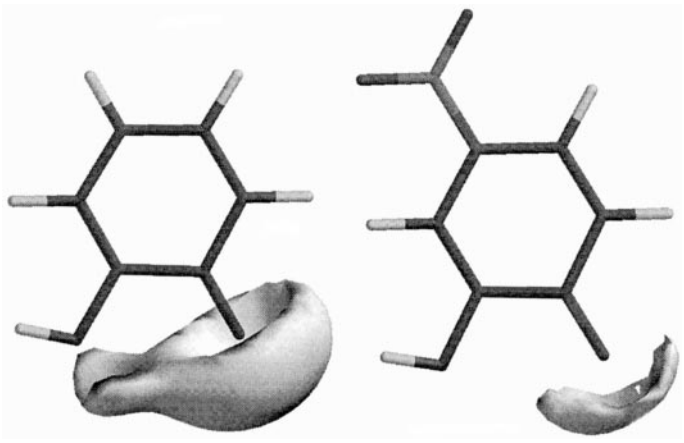

Fig. 3. The molecular electrostatic isoenergy surfaces plotted at −160 kcal/mol for catechol (left) and 4-nitrocatechol.

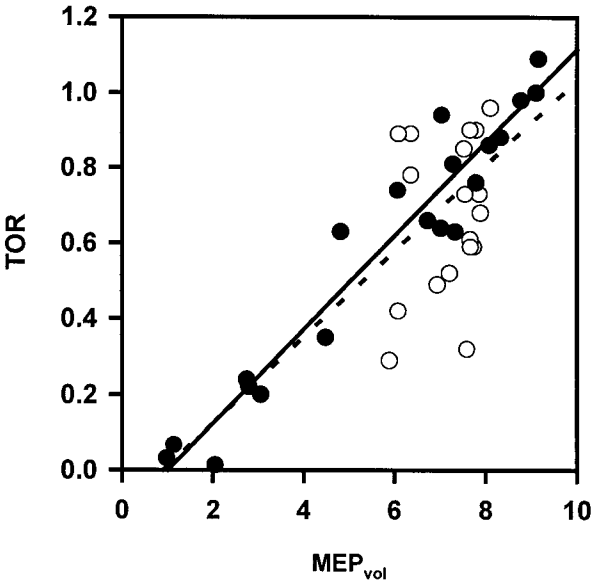

Fig. 4. Correlation between relative turn-over rates (TOR) and volumes (Å^3) of the isoenergy surface of molecular electrostatic potential (MEP$_{vol}$) calculated at −160 kcal/mol for the catecholate monoanion with the higher MEP minimum. The lines represent linear regression for catechols with nonionized substituents (●) and the whole data set (dashed line).

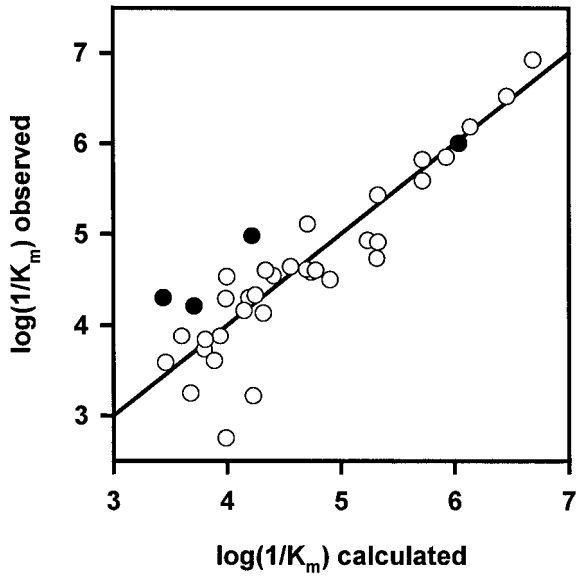

Fig. 5. Correlation between observed and calculated log(1/K_m) values (● pyrogallol derivatives).

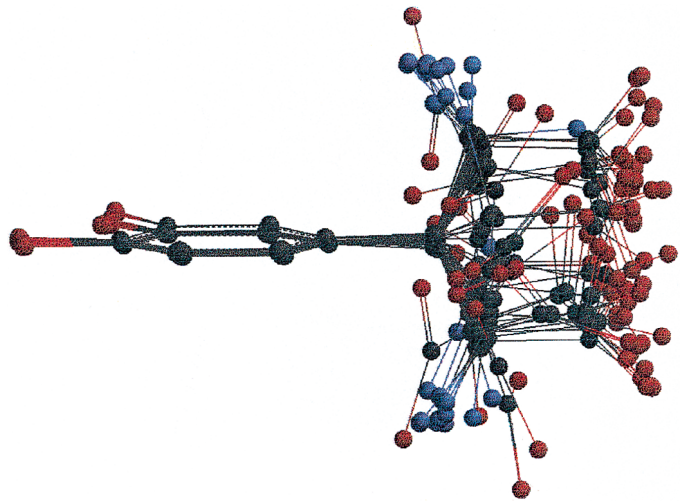

Fig. 6. Low-energy conformations (AM1) of dopamine and hydrocaffeic acid. Nitrogen atoms are shown as blue balls and oxygen atoms as red balls. Hydrogens are omitted for clarity.

tion: nitro-group in the *ortho*-position to the ionized hydroxyl and conjugated carboxyl group. The observed turnover rates in these cases were in accordance with the expected effect of the substituents on the acidity of the catechol hydroxyls. The failure of MEP parameters in the two cases is probably related to limited applicability of gas phase calculations in predicting solution properties. Poor steric fit was found to be the second factor causing a significant lowering of the methylation rate. Lowered turnover rate (TOR < 0.6) was observed for all compounds overlapping with AdoMet, the catalytic loop Trp143-Lys144, or simultaneously the two "gate keeper" residues Pro174 and Trp38 in all accessible conformations. The mechanisms of lowering the rate are probably the steric hindrance for positioning the reacting atom in the case of low affinity polar compounds, and changing the geometry of the reaction center in the case of hydrophobic compounds with higher binding energies. Apomorphine, overlapping heavily with AdoMet, inhibited the reaction completely.

The third mechanism proposed to affect catalysis, electrostatic interference with the reaction center, was found in the case of only one compound, 2,3-dihydroxybenzoic acid. Fitting in the crystal structure suggests that one of the negatively charged oxygens is in contact with the positively charged methyl group of AdoMet and close to the amino group of the catalytic base, Lys144.

Electron withdrawing substituent effect was the most important factor lowering K_m values. This was expected based on earlier QSAR studies of catechol-type COMT inhibitors (Taskinen et al., 1989; Lotta et al., 1992). The equation above (under *Factors Governing Reactivity and Affinity*) can be used to predict K_m values for compounds with reasonable steric fit, provided that the groups that determine the $\log K_{ow}$ interact with the binding site. Whole-molecule hydrophobicity can predict the effect of hydrophobic and polar interactions only in the statistical sense. In the case of individual molecules, the effect depends on the shape of the hydrophobic surfaces, location of polar groups in rigid structures, and the allowed or favored conformations in the case of flexible structures. Therefore, modeling in the crystal structure should complement prediction of K_m values using the regression model.

All factors found to affect K_m values are not taken into account in the above equation. Hydroxyl groups and ionic groups that are fixed close to the binding pocket walls, or have limited freedom to escape contact because of steric crowding, showed a tendency to lower affinity with the exception of hydroxyl group in the 3-position. Surprisingly, the third hydroxyl increased affinity severalfold (Fig. 5). The binding free energy gain resulting from an extra hydrogen bond donor is not expected to be large because of the energy cost of desolvation, even though a new hydrogen bond is formed in the bound state. In this case, no hydrogen bonding partner can be identified in the active site crystal structure. It is possible to construct a statistically significant QSAR model with an indicator parameter for the third adjacent hydroxyl. This equation has coefficient of about 0.5 for the indicator, suggesting that, on average, pyrogallol derivatives have $\log(1/K_m)$ values increased by 0.5 log units. Even steric effects could be described with a statistically significant parameter. However, the predictive ability of multiparameter models cannot be validated with the data available.

The specificity of different catechols can be compared with the use of specificity constants $k_A = k_{cat}/K_m$, which determine the ratio of rates of competing substrates, when they are mixed together (Cornish-Bowden, 1995). The relative specificity constants $k_{A(rel)}$ were obtained as the ratio of V_{max}/K_m values taking $V_{max} = k_{cat} \times$ [enzyme concentration]. The same structural factor, electronegativity of substituents, can cause lowering of values for both k_{cat} and K_m. Because of the combined effect, certain catechols with poor reactivity seemed to be the most specific substrates. Best substrates with both high k_A value and high turnover rate were catechols containing a hydrophobic 4,5-fused ring, such as 2,3-dihydroxynaphthalene and 2-hydroxyestradiol, or a conjugated, planar, nonelectron-withdrawing substituent, such as caffeic acid. The latter compound is found in high concentration in coffee beans. Interestingly, recent reports suggest that coffee may lower the risk of Parkinson's disease (Ross et al., 2000).

Dobutamine and benserazide seemed to be the most specific COMT substrates of the clinically used drugs studied. In the new triple therapy of Parkinson's disease, L-DOPA is coadministered with a DDC inhibitor and a COMT inhibitor. The DDC inhibitor benserazide seemed to be 15 times more specific than L-DOPA, which is the target of COMT inhibition, whereas the alternative DDC inhibitor, carbidopa, was two times less specific. Differences found in the COMT-catalyzed methylation of carbidopa and benserazide are in agreement with previous in vitro results obtained using purified COMT from pig liver (Hagan et al., 1980, Gordonsmith et al., 1982). Molecular reasons for the different behavior of the DDC inhibitors are obvious from the discussion above. Benserazide is a pyrogallol derivative. Polar effects of its flexible side chain are balanced by the favorable effect of the third adjacent hydroxyl. The K_m value of benserazide is actually close to that of 5-hydroxydopamine, the pyrogallol analog of dopamine.

MB-COMT has a primary structure identical with that of S-COMT, but has a 50 amino-acid amino-terminal extension, presumably for anchoring the protein in the membrane. Certain kinetic differences between S-COMT and MB-COMT, such as a lower K_m value of MB-COMT for dopamine, are well established (Rivett and Roth, 1982; Lotta et al., 1995). The differences may be caused by the membrane or by folding the extension close to the active site. Our ongoing work aims to elucidate the structure-reactivity relationships of MB-COMT.

In summary, several molecular mechanisms controlling the methylation by human S-COMT were identified. The structure-activity relationships found allow the prediction of reactivity, affinity and specificity with useful accuracy for catechol compounds with a wide range of structures and properties. The knowledge can be utilized in the evaluation of metabolic interactions of endogenous catechols, drugs and dietary catechols, and in the designing of new COMT inhibitors (e.g., centrally acting) or other drugs with the catechol pharmacophore (e.g., DDC inhibitors or dopamine agonists) with controlled COMT interaction.

Acknowledgments

Mrs. Raija Savolainen and Mr. Jarmo Huuskonen are gratefully acknowledged for skillful technical assistance.

References

Bertocci B, Miggiano V, Da Prada M, Dembic Z, Lahm H-W and Malherbe P (1991) Human catechol-*O*-methyltransferase: Cloning and expression of the membrane-associated form. *Proc Natl Acad Sci USA* **88:**1416–1420.

Bradford M (1976) A rapid and sensitive method for the quantitation of microgram quantities of protein utilizing the principle of protein dye binding. *Anal Biochem* **72:**248–254.

Cornish-Bowden A (1995) *Fundamentals of Enzyme Kinetics*, pp 105–108, Portland Press, London.

Eisenhofer G, Keiser H, Friberg P, Mezey E, Huynh T-T, Hiremagalur B, Ellingson T, Duddempudi S, Eijsbouts A and Lenders WM (1998) Plasma metanephrines are markers of pheochromocytoma produced by catechol-O-methyltransferase with tumors. *J Clin Endocrin Metab* **83:**2175–2185.

Gordonsmith RH, Raxworthy MJ and Gulliver PA (1982) Substrate stereospecificity and selectivity of catechol-*O*-methyltransferase for DOPA, DOPA derivatives, and α-substituted catecholamines. *Biochem Pharmacol* **31:**433–437.

Hagan RM, Raxworthy MJ and Gulliver PA (1980) Benserazide and carbidopa as substrates of catechol-*O*-methyltransferase: New mechanism of action in Parkinson's disease. *Biochem Pharmacol* **29:**3123–3126.

Keränen T, Gordin A, Harjola V-P, Karlsson M, Korpela K, Pentikäinen PJ, Rita H, Seppälä L and Wikberg T (1993) The effect of catechol-*O*-methyltransferase inhibition by entacapone on the pharmacokinetics and metabolism of levodopa in healthy volunteers. *Clin Neuropharmacol* **16:**145–156.

Kuhn B and Kollman PA (2000) QM-FE and molecular dynamics calculations on catechol O-methyltransferase: Free energy of activation in the enzyme and in aqueous solution and regioselectivity of the enzyme-catalyzed reaction. *J Am Chem Soc* **122:**2586–2596.

Lau EY and Bruice TC (1998) Importance of correlated motions in forming highly reactive near attack conformations in catechol *O*-methyltransferase. *J Am Chem Soc* **120:**12387–12394.

Lautala P, Ulmanen I and Taskinen J (1999) Radiochemical high-performance liquid chromatographic assay for the determination of catechol *O*-methyltransferase activity towards various substrates. *J Chromatogr Br* **736:**143–151.

Lotta T, Taskinen J, Bäckström R and Nissinen E (1992) PLS modelling of structure-activity relationships of catechol *O*-methyltransferase inhibitors. *J Comput Aided Mol Des* **6:**253–272.

Lotta T, Vidgren J, Tilgmann C, Ulmanen I, Melén K, Julkunen I and Taskinen J (1995) Kinetics of human soluble and membrane-bound catechol *O*-methyltransferase: A revised mechanism and description of the thermolabile variant of the enzyme. *Biochemistry* **34:**4202–4210.

Lundström K, Salminen M, Jalanko A, Savolainen R and Ulmanen I (1991) Cloning and characterization of human placental catechol-*O*-methyltransferase cDNA. *DNA Cell Biol* **10:**181–189.

Lundström K, Tilgmann C, Peränen J, Kalkkinen N and Ulmanen I (1992) Expression of enzymatically active rat liver and human placental catechol-*O*-methyltransferase in *Escherichia coli*; purification and partial characterization of the enzyme. *Biochim Biophys Acta* **1129:**149–154.

Malherbe P, Bertocci B, Caspers P, Zürcher G and Da Prada M (1992) Expression of functional membrane-bound and soluble catechol-*O*-methyltransferase in *Escherichia coli* and a mammalian cell line. *J Neurochem* **58:**1782–1789.

Meylan WM and Howard PH (1995) Atom/fragment contribution method for estimating octanol-water partition coefficients. *J Pharm Sci* **84:**83–92.

Männistö PT, Ulmanen I, Lundström K, Taskinen J, Tenhunen J, Tilgmann C and Kaakkola S (1992) Characteristics of catechol O-methyltransferase (COMT) and properties of selective COMT inhibitors, in *Progress in Drug Research* (Jucker E ed) pp 291–350, Birckhäuser Verlag, Basel.

Ovaska M and Yliniemelä A (1998) A semiempirical study on inhibition of catechol *O*-methyltransferase by substituted catechols. *J Comput Aided Mol Des* **12:**301–307.

Perrin DD, Dempsey B and Serjeant EP (1981) *pKa Predictions for Organic Acids and Bases*, Chapman and Hall, London.

Rivett AJ and Roth JA (1982) Kinetic studies on the O-methylation of dopamine by human brain membrane-bound catechol *O*-methyltransferase. *Biochemistry* **21:**1740–1742.

Ross GW, Abbot RD, Petrovitch H, Morens DM, Grandinetti A, Tung K-H, Tanner CM, Masaki KH, Blanchette BL, Curb JD, Popper JS and White LR (2000) Association of coffee and caffeine intake with the risk of Parkinson disease. *JAMA* **283:**2674–2679.

Salminen M, Lundström K, Tilgmann C, Savolainen R, Kalkkinen N and Ulmanen I (1990) Molecular cloning and characterization of rat liver catechol-*O*-methyltransferase. *Gene* **93:**241–247.

Taskinen J, Vidgren J, Ovaska M, Bäckström R, Pippuri A and Nissinen E (1989) QSAR and binding model for inhibition of rat liver catechol-O-methyl-transferase by 1,5-substituted-3,4-dihydroxybenzenes. *Quant Struct-Act Relat* **8:**210–213.

Tenhunen J, Salminen M, Lundström K, Kiviluoto T, Savolainen R and Ulmanen I (1994) Genomic organization of the human catechol *O*-methyltransferase gene and its expression from two distinct promoters. *Eur J Biochem* **223:**1049–1059.

Tilgmann C, Melén K, Lundström K, Jalanko A, Julkunen I, Kalkkinen N and Ulmanen I (1992) Expression of recombinant human soluble and membrane-bound catechol *O*-methyltransferase in eukaryotic cells and identification of the respective enzymes in rat brain. *Eur J Biochem* **207:**813–821.

Tilgmann C and Ulmanen I (1996) Purification methods of mammalian catechol-*O*-methyltransferases. *J Chromatogr Br* **684:**147–161.

Ulmanen I, Peränen J, Tenhunen J, Tilgmann C, Karhunen T, Panula P, Bernasconi L, Aubry J-P and Lundström K (1997) Expression and intracellular localization of catechol *O*-methyltransferase in transfected mammalian cells. *Eur J Biochem* **243:**452–459.

Vidgren J, Svensson LA and Liljas A (1994) Crystal structure of catechol. *O*-methyltransferase *Nature (Lond)* **368:**354–358.

Zheng Y-J and Bruice TC (1997) A theoretical examination of the factors controlling the catalytic efficiency of a transmethylation enzyme: Catechol *O*-methyltransferase *J Am Chem Soc* **119:**8137–8145.

Zürcher G, Dingemanse J and Da Prada M (1993) Potent COMT inhibition by Ro 40–7592 in the periphery and in the brain. *Adv Neurol* **60:**641–647.

Send reprint requests to: Dr. Jyrki Taskinen, Department of Pharmacy, Division of Pharmaceutical Chemistry, University of Helsinki, P.O. Box 56, FIN-00014, Finland. E-mail: jyrki.taskinen@helsinki.fi